

# Population synthesis of wide binary millisecond pulsars

B. Willems\* and U. Kolb\*

*Department of Physics and Astronomy, The Open University, Walton Hall, Milton Keynes, MK7 6AA, UK*

Accepted ... Received ...; in original form ...

## ABSTRACT

Four evolutionary channels leading to the formation of wide binary millisecond pulsars are investigated. The majority of binary millisecond pulsars are found to descend from systems in which the most massive component undergoes a common-envelope phase prior to the supernova explosion leading to the birth of the neutron star.

The orbital period distribution of simulated samples of wide binary millisecond pulsars is compared with the observed distribution of Galactic binary millisecond pulsars for a variety of parameters describing the formation and evolution of binaries. The distribution functions typically show a short-period peak below 10 days and a long-period peak around 100 days. The observed distribution is best reproduced by models with highly non-conservative mass transfer, common-envelope efficiencies equal to or larger than unity, a critical mass ratio for the delayed dynamical instability larger than 3, and no or moderate supernova kicks at the birth of the neutron star. Few systems are found with orbital periods longer than 200 days, irrespective of the accretion efficiency of neutron stars. This occurs as a result of the upper limit on the initial orbital periods beyond which the binary avoids the common-envelope phase prior to the supernova explosion of the primary.

**Key words:** binaries: general – stars: evolution – stars: neutron – stars: white dwarfs – pulsars: general – methods: statistical

## 1 INTRODUCTION

In close binaries containing a neutron star, the evolution of the system is driven by the nuclear evolution of the companion and the loss of angular momentum through processes as magnetic braking and gravitational radiation. When the combination of these processes causes the companion to fill its Roche lobe, mass and angular momentum are transferred to the neutron star which is then spun up to form a recycled pulsar, unless transient behaviour prevents effective accretion. At the end of the mass-transfer phase, the binary emerges as a binary millisecond pulsar (BMSP) consisting of a rapidly rotating neutron star in a nearly circular orbit around a low-mass white dwarf, which used to be the core of the Roche-lobe overflowing companion (for a review see Bhattacharya & van den Heuvel 1991, Phinney & Kulkarni 1994). If the mass transfer phase takes place during the companion's ascent of the red giant branch, the relation between the core mass and the radius of the star and the relation between the Roche-lobe radius and the orbital separation, lead to a correlation between the orbital period of the BMSP and the mass of the white dwarf. This correlation has been studied extensively by Joss, Rappaport & Lewis (1987), Savonije

(1987), Rappaport et al. (1995), Ritter (1999), and Tauris & Savonije (1999).

The precise evolutionary path followed by a BMSP progenitor depends mainly on the orbital period and on the mass of the donor star at the onset of Roche-lobe overflow after the supernova explosion of the primary. Systems with orbital periods longer than  $\sim 20$  days and donors more massive than  $\sim 2.0 M_{\odot}$  are likely to evolve through a common-envelope phase during which the envelope of the donor is expelled and the neutron star spirals in towards the donor star's core (Kalogera & Webbink 1998). If the orbital period is shorter, the common-envelope phase can be avoided for donor stars up to  $\sim 4.0 M_{\odot}$  (Tauris, van den Heuvel & Savonije 2000; Kolb et al. 2000; Podsiadlowski, Rappaport & Pfahl 2002). Binaries with donor stars less massive than  $\sim 2.0 M_{\odot}$  will become low-mass X-ray binaries, for which the evolution depends on whether the orbital period is longer or shorter than the bifurcation period separating diverging from converging systems (Pylyser & Savonije 1988, 1989). Only low-mass X-ray binaries with orbital periods longer than the bifurcation period will eventually evolve into wide BMSPs.

At present, 33 BMSPs with orbital periods longer than one day have been found in the Galactic disc. Their orbital periods, eccentricities, and white dwarf masses are listed in Table 1 (Ritter, private communication). Inspection of the

\* E-mail: B.Willems@open.ac.uk, U.C.Kolb@open.ac.uk

**Table 1.** Observed orbital periods, eccentricities, and white dwarf masses of Galactic BMSPs with orbital periods longer than 1 day. The data is derived from Taam et al. (2000) with updated information from Ritter (private communication).

Name	$P_{\text{orb}}$ (days)	$e$	$M_{\text{WD}}/M_{\odot}$
J0613-0200	1.19851	0.000007	>0.13
J1435-6100	1.35489	0.000010	>0.90
J0034-0534	1.58928	<0.00002	>0.15
J0218+4232	2.02885	<0.00002	>0.16
J2317+1439	2.45933	0.0000005	
J1911-1114	2.71656	<0.000013	>0.12
J1157-5112	3.50739	0.000402	>1.18
J1045-4509	4.08353	0.000024	>0.16
J1745-0952	4.94345	0.000018	>0.11
J1732-5049	5.26300	0.000001	0.18
J0437-4715	5.74104	0.000019	0.22-0.32
J1603-7202	6.30863	<0.00002	>0.29
J2129-5721	6.62549	<0.000017	>0.14
J2145-0750	6.83890	0.000018	>0.43
J1022+1001	7.80513	0.000098	>0.73
J0621+1002	8.31868	0.002458	>0.45
J1518+4904	8.63400	0.249485	
J1918-0642	10.91318	0.000022	>0.24
J1804-2717	11.12871	0.000035	>0.21
B1855+09	12.32717	0.000027	0.24-0.29
J1454-5846	12.42307	0.001898	>0.87
J1810-2005	15.01220	0.000025	>0.28
J1709+23	22.7		
J1618-3919	22.8		
J2033+17	56.2	<0.05	>0.2
J1713+0747	67.82513	0.000075	>0.27
J1455-3330	76.17458	0.000167	>0.27
J2019+2425	76.51163	0.000111	0.33
J2229+2643	93.01589	0.000256	
J1643-1224	147.01740	0.000506	>0.13
B1953+29	117.34910	0.000330	
J1640+2224	175.46066	0.000797	

observed orbital periods shows a paucity of systems with periods between 30 and 60 days, and an absence of systems with periods longer than 200 days. A theoretical interpretation of the possible period gap was given by Tauris (1996) and Taam, King & Ritter (2000), while an explanation for the upper limit was put forward by Ritter & King (2002).

With this paper, we initiate a systematic study based on population synthesis techniques to investigate the different evolutionary channels leading to the formation of wide BMSPs and to compare the theoretical with the observed orbital period distribution of wide BMSPs. We particularly investigate whether a set of standard evolutionary parameters can be found to reproduce the observed orbital period distribution without including observational selection effects or pulsar lifetime issues. Due to the large uncertainties involved in the determination of the masses of the white dwarfs in the observed BMSPs (see Table 1) we presently do not consider the white dwarf mass distribution as good a tool as the orbital period distribution to confine stellar and binary evolution and formation parameters.

Since BMSPs located in globular clusters are thought to be formed through tidal encounters of neutron stars with primordial binaries (e.g. Rappaport, Putney & Verbunt 1989), we limit ourselves to BMSPs in the Galactic disc. We also

leave aside systems with orbital periods shorter than 1 day since they are likely to follow evolutionary paths different from those of the BMSPs investigated here. In particular, the evolution of the short-period systems is dominated by angular momentum losses for which quantitative descriptions are still uncertain (Ergma & Sarna 1996; Kalogera, Kolb & King 1998; Ergma, Sarna & Antipova 1998; Rasio, Pfahl & Rappaport 2000; Dewi et al. 2002; and in particular Podsiadlowski et al. 2002 and references therein).

The plan of the paper is as follows. In Sect. 2, we briefly summarise the basic concepts of the binary evolution code used in this investigation. In Sect. 3, the evolutionary channels leading to the formation of wide BMSPs are discussed. In Sect. 4, we explore the parameter space occupied by the BMSP progenitors during various phases of their evolution. The effects of the input parameters adopted in our binary evolution calculations on the orbital period distribution of wide BMSPs and the relative contributions of the different formation channels to the total population of wide BMSPs are investigated in Sect. 5. The final section is devoted to concluding remarks.

## 2 THE BINARY EVOLUTION CODE

### 2.1 Single star evolution

We developed a rapid binary evolution code based on the analytical approximations for the evolution of single stars with masses ranging from 0.1 to 100  $M_{\odot}$  and metallicities between  $Z = 0.0001$  and  $Z = 0.03$  derived by Hurley, Pols & Tout (2000). The formulae express the luminosity, radius, and core mass of a star as a function of its age, mass, and metallicity for all phases from the zero-age main sequence up to and including the remnant stages. For massive stars ending their life as a neutron star, we simplified the prescription for the mass of the remnant so that all neutron stars are born with a mass of 1.4  $M_{\odot}$ . The simplification is justified by the fact that most neutron stars with accurately known masses have a mass close to this value (Thorsett & Chakrabarty 1999). We furthermore limit ourselves to Population I stellar compositions.

The single star evolution scheme takes into account mass loss from the envelope due to stellar winds. Stars beyond the main sequence are subjected to the mass-loss rates given by Kudritzki & Reimers (1978), the superwind phase on the asymptotic giant branch (AGB) is modelled using the prescription of Vassiliadis & Wood (1993), massive stars are subjected to mass loss over the entire Hertzsprung-Russell diagram as outlined by Nieuwenhuizen & De Jager (1990) and Kudritzki et al. (1989), and naked helium stars are subjected to a Wolf-Rayet-type mass-loss rate. For more details, we refer to Hurley et al. (2000).

In addition to the stellar evolution of the binary components, we also take into account the evolution of the binary configuration due to gravitational radiation, magnetic braking, mass loss and accretion from stellar winds, and conservative or non-conservative Roche-lobe overflow. For the implementation of magnetic braking, we adopt a Skumanich-type parametrisation modified to take into account the dependency on the mass of the convective envelope as described by Hurley et al. (2000). We furthermore

assume the orbit of the binary to be circular and keep the rotation of the stars synchronised with their orbital motion at all times. The recipe followed for the implementation of the binary evolution is essentially along the lines laid down by Hurley, Tout & Pols (2002). In the following paragraphs we therefore restrict ourselves to summarising the points where our treatment deviates from the outline given by these authors.

## 2.2 Roche-lobe overflow

When the combined effects of stellar and orbital evolution cause a component of a close binary to become larger than its Roche lobe, mass is transferred from the Roche-lobe overflowing star to the companion. The stability of the mass transfer process depends on the adiabatic and thermal radius-mass exponents,  $\zeta_{\text{ad}}$  and  $\zeta_{\text{th}}$ , and the Roche-lobe index  $\zeta_{\text{L}}$  (for a definition see, e.g., Webbink 1985). For stars on the main sequence or in the Hertzsprung gap, we use the tabulated values for  $\zeta_{\text{ad}}$  and  $\zeta_{\text{th}}$  given by Hjellming (1989). In all other cases we adopt the prescription given by Hurley et al. (2002). For the determination of the Roche-lobe index  $\zeta_{\text{L}}$ , we follow the procedure outlined by Kolb et al. (2001).

If mass transfer proceeds on either the nuclear ( $\zeta_{\text{L}} < \zeta_{\text{ad}}$  and  $\zeta_{\text{L}} < \zeta_{\text{eq}}$ ) or the thermal ( $\zeta_{\text{eq}} < \zeta_{\text{L}} < \zeta_{\text{ad}}$ ) timescale of the Roche-lobe overflowing star, the companion is assumed to accrete a fraction  $1 - \gamma$  of the transferred mass determined by the ratio of the mass-transfer timescale to the accretor's thermal timescale (for details see Hurley et al. 2002). The remaining fraction is assumed to be expelled from the system, carrying away the specific orbital angular momentum of the companion. In the particular case of a neutron star accretor, an average accretion rate is determined by imposing an upper limit of  $(\Delta M_{\text{NS}})_{\text{max}}$  on the amount of mass that can be accreted (for details see Appendix A). Once this limit has been reached, mass accretion onto the neutron star is switched off completely to ensure that the neutron star accretes no more than  $(\Delta M_{\text{NS}})_{\text{max}}$ . We impose this upper limit to mimic the low accretion efficiency neutron stars are thought to have (e.g. King & Ritter 1999, Ritter & King 2002). In addition, we also limit the mass-accretion rate to the Eddington rate at all times.

In the case of dynamically unstable mass transfer ( $\zeta_{\text{ad}} < \zeta_{\text{L}}$ ) from a giant-like star, the binary is assumed to enter a common-envelope phase during which the orbital separation is reduced and the envelope is ejected from the system. The phase is modelled by equating the binding energy of the giant's envelope to the change in orbital energy of the two stars:

$$\frac{G(M_c + M_e)M_e}{\lambda R_{\text{L}}} = \alpha \left[ \frac{G M_c M_2}{2 a_{\text{f}}} - \frac{G(M_c + M_e)M_2}{2 a_{\text{i}}} \right]. \quad (1)$$

In this equation,  $G$  is the gravitational constant,  $M_c$  and  $M_e$  are the core and envelope mass of the Roche-lobe overflowing star,  $R_{\text{L}}$  is the radius of the donor star's Roche lobe,  $M_2$  is the mass of the companion,  $a_{\text{i}}$  and  $a_{\text{f}}$  are the orbital separations of the binary at the start and at the end of the common-envelope phase,  $\lambda$  is a dimensionless structure parameter determining the binding energy of the giant's envelope, and  $\alpha$  is the fraction of the orbital energy that is transferred to the envelope. The parameters  $\lambda$  and  $\alpha$  are usually assumed to be constant and equal to 0.5 and 1.0,

respectively (e.g. de Kool 1992, Politano 1996). In fact, the value of  $\lambda$  depends on the evolutionary stage of the donor star at the onset of the mass-transfer phase (Dewi & Tauris 2000, 2001). However, since no elaborate set of  $\lambda$ -values has been published for the full range of stellar masses considered in our investigation, we here treat  $\lambda$  as a constant.

## 2.3 Supernova explosions

Whenever a component of a close binary undergoes a supernova explosion leading to the birth of a neutron star, we use the expressions established by Kalogera (1996) to derive the post-supernova orbital parameters. If the birth of the neutron star is accompanied by a kick, we assume its magnitude  $v_{\text{kick}}$  to be distributed according to the Maxwellian distribution

$$P(v_{\text{kick}}) = \sqrt{\frac{2}{\pi}} \frac{v_{\text{kick}}^2}{\sigma^3} \exp\left(-\frac{v_{\text{kick}}^2}{2\sigma^2}\right), \quad (2)$$

where  $\sigma$  is the dispersion of the kick velocities. If the supernova explosion causes the binary to become eccentric, we instantaneously circularise the orbit while conserving the total orbital angular momentum of the binary.

## 3 EVOLUTIONARY CHANNELS

Before proceeding to the statistics of the BMSP population and the effects of the various assumptions made in our treatment of stellar and binary evolution and formation, we explore the different evolutionary channels leading to the formation of wide BMSPs.

We followed the evolution of a large number of binaries starting with zero-age main sequence components up to a maximum evolutionary age of 15 Gyr. The initial masses of the binary components are taken in the interval between  $0.1 M_{\odot}$  and  $60 M_{\odot}$ , and the initial orbital periods in the range from 10 to 10 000 days. We used equidistantly spaced grids consisting of 40 grid points for the logarithm of the initial masses and 200 grid points for the logarithm of the initial periods. For symmetry reasons only binaries with  $M_1 > M_2$  are evolved. Each time a supernova explosion leads to the birth of a neutron star, 200 random kick velocities are generated and the evolution of the surviving binaries is followed until the imposed age limit of 15 Gyr. In order to identify as many formation channels as possible, we do not apply any weighting to the initial masses and the initial orbital periods at this stage. The weighted contributions of the different formation channels to the population of wide BMSPs will be discussed in Sect. 5.

For the results presented in this section, a standard set of input parameters was adopted for the binary evolution calculations: common-envelope phases are modelled using the values  $\lambda = 0.5$  and  $\alpha = 1.0$  for the binding-energy parameter and the envelope-ejection efficiency, the occurrence of a delayed dynamical instability is determined using the values tabulated by Hjellming (1989), supernova kicks are generated with a Maxwellian velocity dispersion  $\sigma = 190$  km/s, and an upper limit  $(\Delta M_{\text{NS}})_{\text{max}} = 0.2 M_{\odot}$  is imposed on the mass that can be accreted by a neutron star.

These assumptions will serve as a reference for the population synthesis calculations presented in Sect. 5, where we will refer to them as model A.

We find four major evolutionary channels leading to the formation of wide BMSPs. In three of these channels, the primary undergoes a common-envelope phase (CE) which ejects the primary’s envelope from the system and reduces the orbital separation. For primaries more massive than  $\sim 20 M_{\odot}$  the common-envelope phase takes place when the primary crosses the Hertzsprung gap, while for primaries less massive than  $\sim 20 M_{\odot}$  the common-envelope phase takes place when the primary ascends the AGB. Both cases lead to similar evolutionary paths. For the continuation of the evolution, it is necessary to distinguish between binaries with low- and intermediate mass secondaries.

The main evolutionary phases of a BMSP progenitor with a low-mass secondary are illustrated in Fig. 1, where the initial orbital period is 1400 days and the binary components have initial masses of  $15 M_{\odot}$  and  $1 M_{\odot}$ . The primary fills its Roche lobe after 14 Myr, at which time a stellar wind has reduced the mass of the primary to  $10.3 M_{\odot}$  and increased the orbital period to  $\sim 2690$  days. The primary exits the common-envelope phase as a massive naked helium star which evolves further until it explodes in a type Ib/c supernova and gives birth to a  $1.4 M_{\odot}$  neutron star. After circularisation of the post-supernova orbit, the binary consists of a  $1.0 M_{\odot}$  main-sequence star which orbits the neutron star in a period of 5.7 days. The binary subsequently evolves as a detached system until the secondary expands and fills its Roche lobe during its ascent of the giant branch. The resulting mass-transfer phase is both dynamically and thermally stable and takes place on the nuclear timescale of the giant star. During this phase, mass accretion spins up the neutron star to high rotation rates until it becomes a recycled pulsar. At the end of the mass-transfer phase, the binary emerges as a wide BMSP consisting of a rapidly rotating neutron star in a 64 day orbit around a  $0.3 M_{\odot}$  helium white dwarf, the former core of the giant star. This formation channel has been discussed previously by Bhattacharya & van den Heuvel (1991) and Phinney & Kulkarni (1994), among others. We will refer to it with the label He N.

For BMSP progenitors with intermediate-mass secondaries, the formation channel becomes a bit more complex. Two possible evolutionary paths are displayed in Figs. 2 and 3, in the case of a binary with an initial orbital period of 1400 days and initial component masses of  $30 M_{\odot}$  and  $3.5 M_{\odot}$ . Again, the primary emerges from the common-envelope phase as a massive naked helium star which gives birth to a  $1.4 M_{\odot}$  neutron star in a type Ib/c supernova explosion. The further evolution depends on the circularised post-supernova orbital separation.

If the post-supernova orbital period is smaller than  $\sim 2.5$  days (Fig. 2), the binary enters a case A thermal-timescale mass-transfer phase after 214 Myr and detaches again after 217 Myr when the donor mass has decreased to  $1.2 M_{\odot}$ . This short thermal-timescale mass-transfer phase is followed by a stable nuclear timescale mass-transfer phase after 939 Myr when the secondary approaches the end of the main sequence. This stable mass transfer phase continues all the way up to the giant branch and leads to the formation of a binary consisting of a rapidly rotating neutron star in a

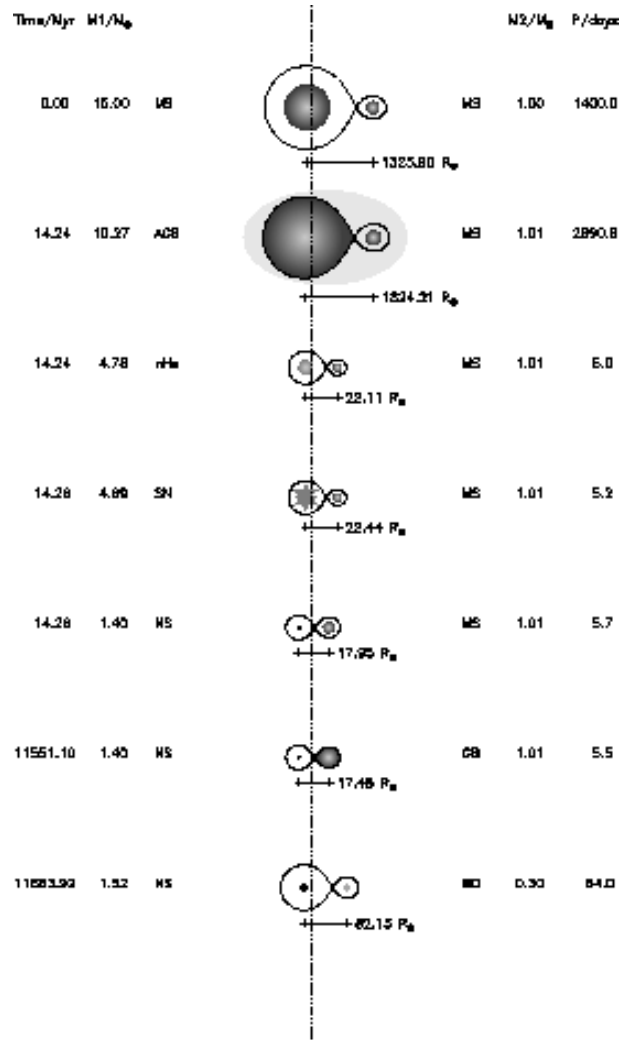


**Figure 1.** The main evolutionary phases of a BMSP progenitor with a low-mass secondary evolving into a helium white dwarf [channel He N]. The two distinguishing phases for this formation channel are the CE phase of the primary prior to the supernova explosion and the stable case B mass-transfer phase after the explosion. The dotted vertical line indicates the mass centre of the binary.

10 day orbit around a  $0.2 M_{\odot}$  helium white dwarf. We label this formation channel He T.

If the post-supernova orbital period is larger than  $\sim 2.5$  days (Fig. 3), the secondary enters a case B thermal-timescale mass-transfer phase when it crosses the Hertzsprung gap. Due to the high mass-transfer rate, the neutron star rejects most of the mass transferred by the companion so that the spin-up process is probably less effective and thus leads to more slowly rotating pulsars than the spin-up process during a slow stable mass-transfer phase (e.g. Li 2002, and references therein). The semi-detached state ends when the hydrogen envelope of the secondary is completely stripped away and its helium core is exposed as a low-mass naked helium star. During the following 135 Myr, the secondary burns helium in the core while a Wolf-Rayet-type stellar wind slowly removes the outer helium layers. The system ends up as a  $0.5 M_{\odot}$  carbon/oxygen white dwarf in

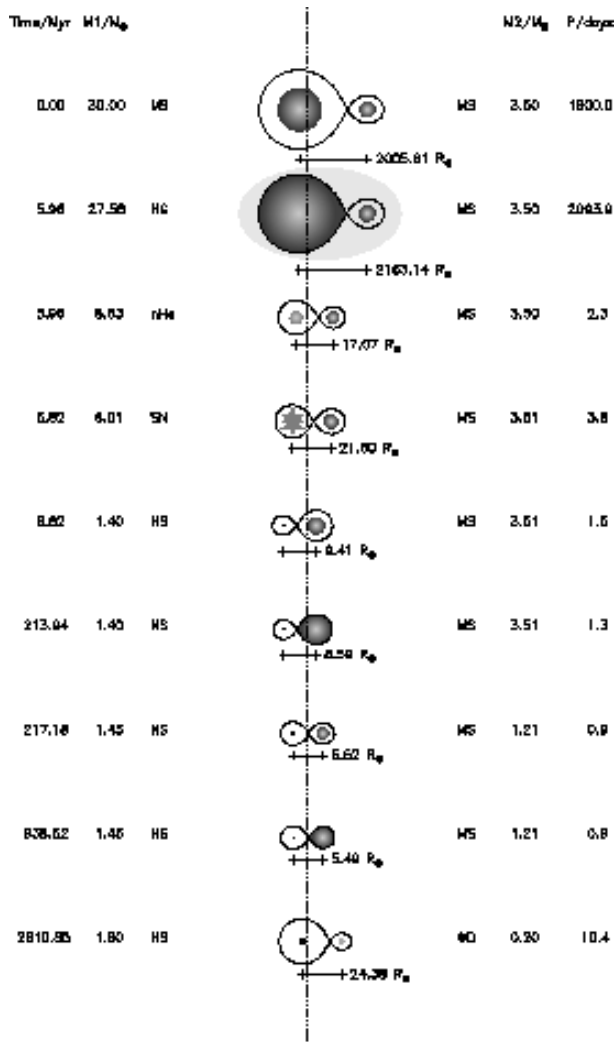


**Figure 2.** As Fig. 1, but with an intermediate-mass secondary evolving into a helium white dwarf [channel He T]. The distinguishing phases are the CE phase of the primary prior to the supernova explosion and the initial thermal-timescale case A mass-transfer phase after the explosion.

a 10.4 day orbit around a neutron star which may or may not be spun up to millisecond periods. This channel was first found independently by King & Ritter (1999) and by Podsiadlowski & Rappaport (2000) [see also Tauris et al. (2000)]. A possible BMSP progenitor that is currently at the end of the early case B mass transfer phase in this channel is the persistent X-ray binary Cygnus X-2 (King & Ritter 1999, Kolb et al. 2000, Podsiadlowski & Rappaport 2000). We will refer to this formation channel with the label CO T.

The fourth and final evolutionary channel for the formation of wide BMSPs corresponds to the direct supernova mechanism discussed by Kalogera (1998). It applies to binaries with low-mass secondaries and initial orbital separations that are wide enough to avoid any kind of Roche-lobe overflow before the supernova explosion of the primary. An example of such a system is displayed in Fig. 4, where the initial orbital period of the binary is 1600 days and the initial masses of the primary and the secondary are  $9 M_{\odot}$  and  $1 M_{\odot}$ , respectively. The wide orbit allows the primary to

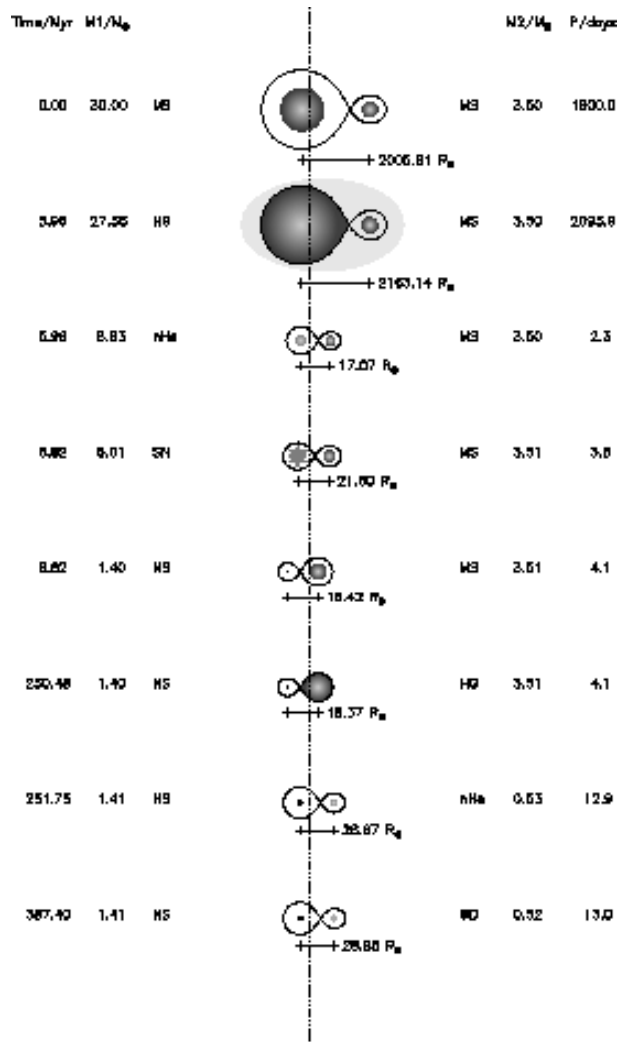


**Figure 3.** Same as Fig. 2, but with a kick velocity such that the secondary evolves into a carbon/oxygen white dwarf [channel CO T]. The distinguishing phases are the CE phase of the primary prior to the supernova explosion and the thermal-timescale case B mass-transfer phase after the explosion.

evolve all the way up to the AGB where it explodes in a type II supernova. After the circularisation of the post-supernova orbit, the binary consists of a  $1.4 M_{\odot}$  neutron star orbiting a fairly unevolved main-sequence star with a long orbital period of 1100 days. The secondary then in turn evolves up to the AGB where it fills its Roche lobe after 12.4 Gyr. At this point, its mass is reduced to  $0.7 M_{\odot}$  due to strong stellar winds on the giant branch and the AGB. The following mass-transfer phase is dynamically and thermally stable, and lasts for about 0.3 Myr. At the end of the mass-transfer phase, the binary consists of a rapidly rotating neutron star in a 1440 day orbit around a  $0.5 M_{\odot}$  carbon/oxygen white dwarf. We label this formation channel CO N.

#### 4 PARAMETER SPACE

Next, we examine the parameter space occupied by systems forming wide BMSPs at the start of their evolution, at the instant just before the supernova explosion of the primary,

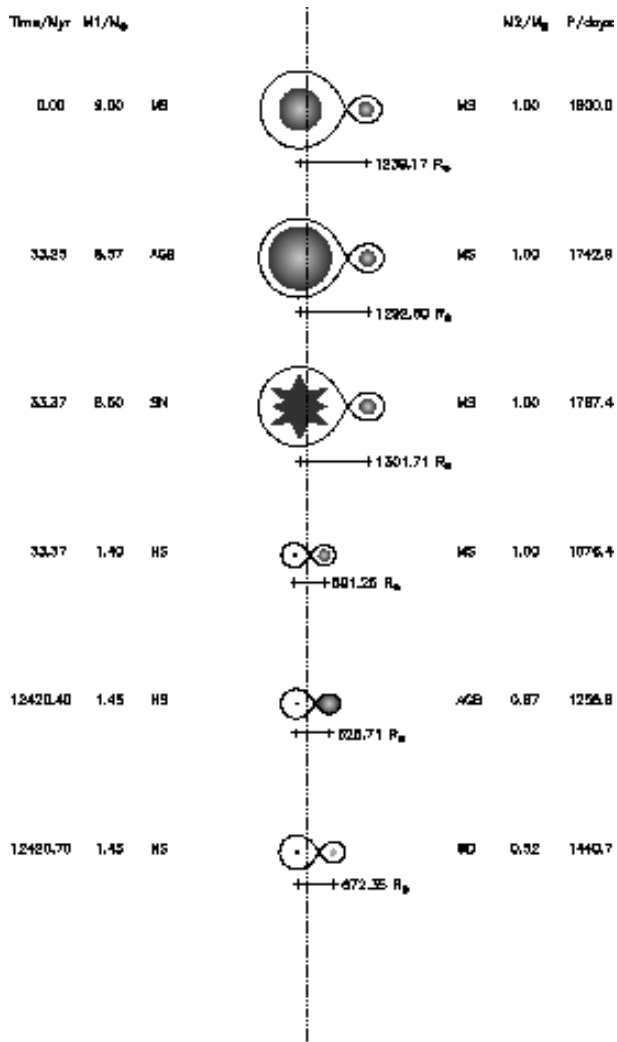


**Figure 4.** As Fig. 1, but with a low-mass secondary evolving into a carbon/oxygen white dwarf [channel CO N]. The distinguishing characteristic is the supernova prior to any interaction between the binary components (see also Kalogera 1998).

at the onset of Roche-lobe overflow after the supernova explosion, and at the birth of the BMSP.

The initial orbital periods  $P_{\text{orb}}$  and secondary masses  $M_2$  of binaries that will evolve into BMSPs are shown in the left-hand panels of Fig. 5. Dark and light dots indicate systems evolving into BMSPs containing a helium white dwarf and systems evolving into BMSPs containing a carbon/oxygen white dwarf, respectively, while big and small dots distinguish between systems undergoing a nuclear or thermal-timescale mass-transfer phase after the supernova explosion of the primary. The bulk of the BMSP progenitors occupy a rather narrow band of orbital periods around 1000 days. The upper limit of the band corresponds to the longest orbital periods for which the primary fills its Roche lobe and undergoes a common-envelope phase prior to its supernova explosion, while the lower limit is formed by the shortest orbital periods for which mergers or contact configurations can be avoided. Besides the band around 1000 days, there is also a small group of systems with orbital periods in the range from 10 to 30 days. These systems evolve along

the same lines as illustrated in Figs. 2 (the He T channel) and 3 (the CO T channel), except that the primary undergoes a rapid thermal-timescale mass-transfer phase instead of a common-envelope phase prior to its supernova explosion. Since these systems do not contribute significantly to the total population of BMSPs we do not consider them separately in our present investigation.

The right-hand panels of Fig. 5 show the orbital periods and secondary masses of the BMSP progenitors just before the supernova explosion of the primary. With the exception of a few rare cases, the orbital separations of the initial binaries are substantially reduced due to the common-envelope phase of the primary. The few systems managing to avoid the common-envelope phase are those evolving through the direct supernova mechanism (Fig. 4, the CO N channel). Their orbital periods have increased slightly with respect to their initial orbital periods due to mass loss from the system caused by the stellar wind of the primary. The systems evolving through the direct supernova mechanism into BMSPs containing a helium white dwarf are included in the He N channel, since their post-supernova evolutionary path is similar to that shown in Fig. 1.

In Fig. 6, we show the parameter space occupied by the progenitors of the wide BMSPs after the supernova explosion of the primary, at the onset of Roche-lobe overflow from the secondary. The lines labelled ZAMS, TMS, and BGB represent the orbital periods at which the secondary would fill its Roche lobe if it was located at the zero-age main sequence, the terminal main sequence, or the base of the giant branch, respectively. The thick lines delimit the different stability regions for mass transfer from the secondary. The dark grey region indicates dynamically unstable or delayed dynamically unstable mass transfer, the light grey region indicates thermal-timescale mass transfer, and the intermediate grey region indicates thermally and dynamically stable mass transfer. For the construction of both thin and thick lines, the mass of the neutron star was assumed to be  $1.4 M_{\odot}$ .

The post-supernova orbital periods of the BMSP progenitors depend on the magnitude of the kick velocity imparted to the neutron star at birth. For secondaries with a mass larger than  $\sim 1.3 M_{\odot}$  the dynamical instability of mass transfer sets an upper limit for the post-supernova orbital period. The lower limit on the orbital periods observed in Fig. 6 is a consequence of the lower limit on the post-common-envelope orbital separations resulting from the requirement that the systems exit the common-envelope phase as detached binaries. Lower and upper limits on the mass of the secondary are caused by the imposed age limit of 15 Gyr and by the delayed dynamical instability. Secondaries with a mass smaller than  $\sim 0.9 M_{\odot}$  evolve too slowly to fill their Roche lobe within 15 Gyr, while for secondaries with a mass larger than  $\sim 4.0\text{--}4.5 M_{\odot}$  the initial thermal-timescale mass-transfer phase will evolve into a dynamically unstable phase shortly after the onset of Roche-lobe overflow.

Furthermore, four groups of systems can be distinguished in Fig. 6, in accordance with the four identified formation channels. Systems evolving into BMSPs containing a helium white dwarf either have low-mass secondaries which enter a stable mass-transfer phase when they cross the Hertzsprung gap or ascend the giant branch (Fig. 1, the He N channel), or intermediate-mass secondaries for which

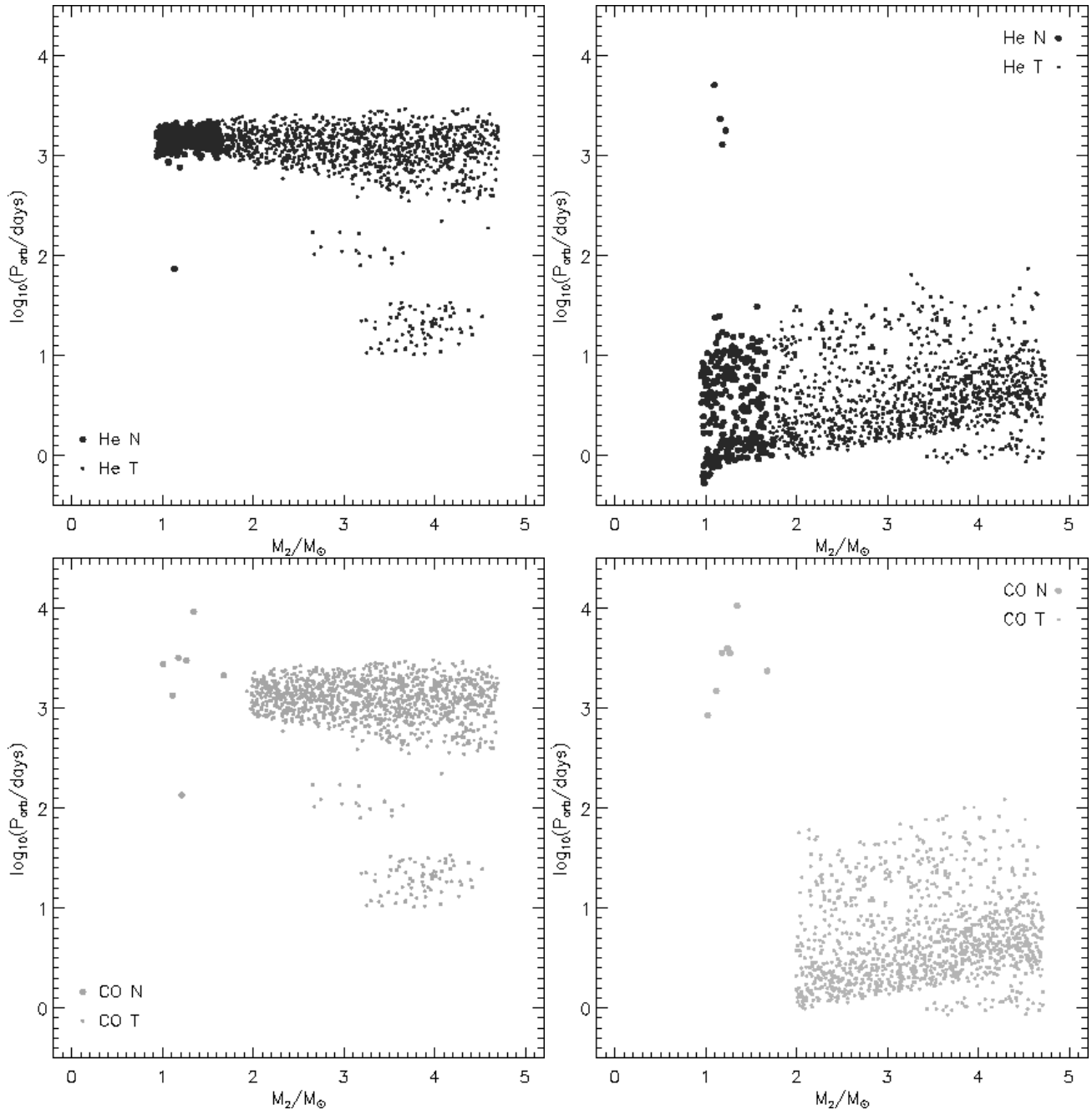


**Figure 5.** The initial (left) and pre-supernova (right) parameter space occupied by the BMSPP progenitors. Small dots represent systems undergoing a thermal-timescale mass-transfer phase after the supernova explosion of the primary, while big dots represent systems for which mass transfer from the secondary is stable at all times. Dark and light dots correspond to systems leading to BMSPPs containing helium and carbon/oxygen white dwarfs, respectively. For clarity, the BMSPPs containing helium and carbon/oxygen white dwarfs are shown in separate panels.

mass transfer initially takes place on a thermal timescale (Fig. 2, the He T channel). Systems evolving into BMSPPs containing a carbon/oxygen white dwarf undergo a thermal-timescale mass-transfer phase when the secondary crosses the Hertzsprung gap (Fig. 3, the CO T channel) or a slow stable mass-transfer phase on the AGB if they manage to avoid the common-envelope phase of the primary prior to the supernova explosion (Fig. 4, the CO N channel).

The parameter space occupied by the BMSPPs in the

$\log P_{\text{orb}} - M_{\text{WD}}$  plane, where  $M_{\text{WD}}$  is the mass of the white dwarf, at the time of their formation is displayed in Fig. 7. The positions of the observed BMSPPs listed in Table 1 are indicated by diamonds. The arrows indicate the uncertainties on the observed white dwarf masses. The orbital periods of the BMSPPs containing helium white dwarfs are correlated with the masses of the white dwarfs. The correlation occurs for both the evolutionary channels He N and He T, and arises due to the relation between the core mass and the ra-

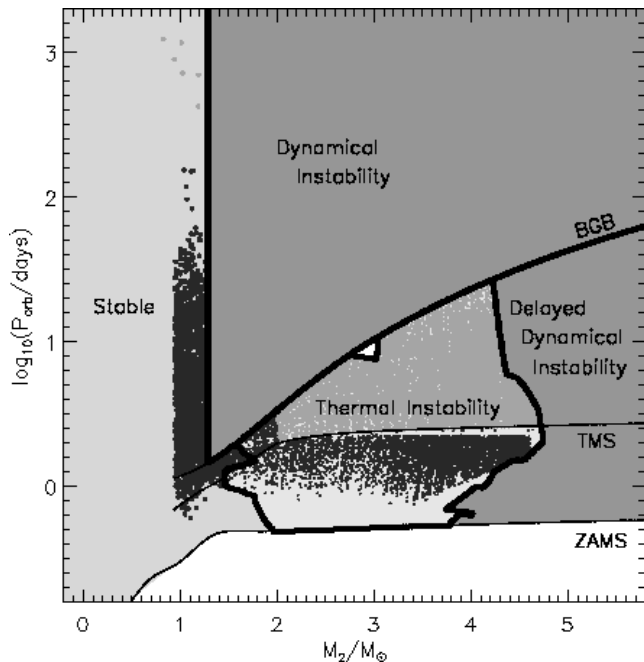


**Figure 6.** The parameter space occupied by the BMSP progenitors at the onset of Roche-lobe overflow from the secondary, after the supernova explosion of the primary. The different dots have the same meaning as in Fig. 5. The thin lines correspond to the orbital periods of a Roche-lobe filling secondary on the zero-age main-sequence (ZAMS), the terminal main-sequence (TMS), and the base of the giant branch (BGB). The thick lines delimit the different stability regions for mass transfer from the secondary. Dark grey indicates dynamically unstable or delayed dynamically unstable mass transfer, light grey indicates thermal-timescale mass transfer, and intermediate grey indicates thermally and dynamically stable mass transfer. For the construction of the thick and the thin lines, the mass of the neutron star was assumed to be  $1.4 M_{\odot}$ .

dius of the giant which is the progenitor of the white dwarf, and due to the relation between the Roche-lobe radius of the giant and the semi-major axis of the orbit (e.g., Rappaport et al. 1995, Tauris & Savonije 1999). The BMSPs forming through the evolutionary channel CO T are located below the systems containing helium white dwarfs, while the ones forming through the direct supernova mechanism CO N form an extension of the  $P_{\text{orb}} - M_{\text{WD}}$  relation for systems containing a helium white dwarf.

We conclude this section by noting that the ranges of orbital periods and secondary masses occupied by the BMSP progenitors at the onset of Roche-lobe overflow after the supernova explosion of the primary and at the formation of the BMSP found from our population synthesis code are in good agreement with those marked out by Tauris et al. (2000) and Podsiadlowski et al. (2002) on the basis of detailed numerical calculations.

## 5 POPULATION SYNTHESIS

### 5.1 Model assumptions

Now that we have established the different formation channels leading to the birth of wide BMSPs and the parameter

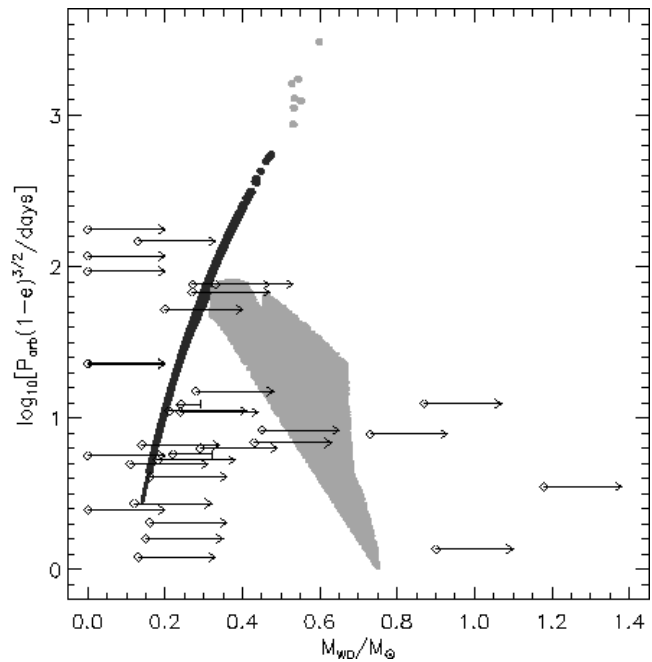


**Figure 7.** The parameter space occupied by wide BMSPs in the  $\log P_{\text{orb}} - M_{\text{WD}}$  plane. The diamonds represent the observed BMSPs listed in Table 1 and the arrows indicate the uncertainties of the observed white dwarf masses. The other symbols have the same meaning as in Fig. 5.

space occupied by their progenitors, we turn our attention to the distribution of the final BMSP orbital periods. In particular, we investigate how the distribution changes with the assumptions made in the binary evolution calculations. We therefore repeated the calculations discussed in the previous sections for a variety of models consisting of different input parameters. Our reference model, model A, corresponds to the input parameters adopted in Sects. 3 and 4. In models CE1 and CE2, the common-envelope efficiency parameter  $\alpha$  is varied. The role of supernova kicks is explored in models K0, KM50, KM100, and KM400: in model K0 no kicks are imparted to the neutron star at birth, while in models KM50, KM100, and KM400, the Maxwellian velocity dispersion takes the values 50, 100, and 400 km/s, respectively. In model NS2, the maximum amount of mass that can be accreted by a neutron star is increased from  $0.2 M_{\odot}$  to  $0.6 M_{\odot}$ . The influence of the critical mass ratio  $q_{\text{c,ddi}}$  for the development of a delayed dynamical instability is investigated in models QCDD and QCDD2. In model C, finally, the limiting case of conservative mass transfer is considered. Details of the differences between the various models are summarised in Table 2.

Each time the evolution of an initial binary leads to the formation of a wide BMSP, its contribution to the orbital period distribution is weighted according to the probability density distributions of its initial parameters. The initial mass of the primary (the initially most massive star) is assumed to be distributed according to the normalised initial mass function

**Table 2.** Population synthesis model parameters.

model	$\alpha$	kicks	$\sigma$ (km/s)	$\gamma_{\text{NS}}$	$q_{\text{c,ddi}}$
A	1.0	yes	190	$1 - 0.2/M_2$	Hjellming (1989)
CE1	0.2	yes	190	$1 - 0.2/M_2$	Hjellming (1989)
CE2	5.0	yes	190	$1 - 0.2/M_2$	Hjellming (1989)
K0	1.0	no	-	$1 - 0.2/M_2$	Hjellming (1989)
KM50	1.0	yes	50	$1 - 0.2/M_2$	Hjellming (1989)
KM100	1.0	yes	100	$1 - 0.2/M_2$	Hjellming (1989)
KM400	1.0	yes	400	$1 - 0.2/M_2$	Hjellming (1989)
NS2	1.0	yes	190	$1 - 0.6/M_2$	Hjellming (1989)
QCDD	1.0	yes	190	$1 - 0.2/M_2$	2.5
QCDD2	1.0	yes	190	$1 - 0.2/M_2$	3.5
C	1.0	yes	190	0	Hjellming (1989)

$$\xi(M_1) = \begin{cases} 0 & M_1/M_\odot < 0.1, \\ 0.38415 M_1^{-1} & 0.1 \leq M_1/M_\odot < 0.75, \\ 0.23556 M_1^{-2.7} & 0.75 \leq M_1/M_\odot < \infty, \end{cases} \quad (3)$$

so that the probability that a star has a mass between  $M_1$  and  $M_1 + dM_1$  is given by  $\xi(M_1) dM_1$ . This distribution function is a simplified version of the initial mass function used by Hurley et al. (2002) and is based on the initial mass function derived by Kroupa, Tout & Gilmore (1993). We recall that for our purpose, we limit ourselves to masses between  $0.1 M_\odot$  and  $60 M_\odot$ .

For a given mass of the primary, the initial mass of the secondary (the initially least massive star) is determined by the mass ratio  $q = M_2/M_1$ . We assume the latter to be distributed according to

$$n(q) = \begin{cases} 1 & 0 < q \leq 1, \\ 0 & q > 1, \end{cases} \quad (4)$$

so that the masses of the component stars are correlated with each other. The existence of such a correlation was suggested, among others, by Eggleton, Fitchett & Tout (1989).

The distribution of the initial orbital separations is assumed to be uniform in the logarithm of the semi-major axis  $a$ . Following Hurley et al. (2002), we adopt the normalised distribution

$$\chi(a) = \begin{cases} 0 & a/R_\odot < 3 \text{ or } a/R_\odot > 10^4, \\ 0.12328 a^{-1} & 3 \leq a/R_\odot \leq 10^4. \end{cases} \quad (5)$$

After weighting the contribution of each newly formed BMSP to the total population, the resulting distribution function is convolved with a constant star-formation rate, on the assumption that the BMSPs under consideration do not evolve any further once they are formed. In particular, we presently do not take into account the spin-down time and thus the finite lifetime of the recycled pulsars. After the convolution, the distribution function is normalised so that the integral over all systems found is equal to one.

## 5.2 The orbital period distribution

We considered the distribution of the orbital periods separately for each of the evolutionary channels discussed in Sect. 3. The most illustrative results are shown in Fig. 8, where the contribution of each channel to the orbital period

distribution is displayed using a different shade of grey. For display purposes, the distribution functions of the BMSPs forming through the evolutionary channel He N are multiplied by a factor of 5, and those of the BMSPs forming through the evolutionary channel CO N by a factor of 100. The orbital period distribution of the observed BMSPs listed in Table 1 is represented by the black solid line.

The orbital period distribution of the BMSPs forming through the He N channel (black) shows a peak between  $\sim 50$  and  $\sim 100$  days, depending on the envelope-ejection efficiency adopted for the common-envelope phase of the primary and on the velocity dispersion adopted for the magnitude of the kick velocity imparted to the neutron star at birth.

A larger envelope-ejection efficiency implies less spiral-in and thus a larger orbital separation at the end of the common-envelope phase. If the binary furthermore survives the subsequent supernova explosion of the primary, the circularised post-supernova orbital separation must be smaller than twice the orbital separation before the supernova explosion (e.g. Kalogera 1996). Increasing the common-envelope efficiency therefore shifts the peak in the orbital period distribution to longer orbital periods. If we identify the peak at long orbital periods in the observed orbital period distribution with the distribution resulting from the He N channel, the best agreement with the observed distribution is found for moderate to large values of the envelope-ejection efficiency ( $\alpha \approx 1.0 - 5.0$ ). An efficiency parameter larger than unity was also suggested by Tauris & Bailes (1996) in an investigation on the origin of the millisecond pulsar velocities and by Tauris & Sennels (2000) in a study on the formation of the binary pulsars PSR B2303+46 and PSR J1141-6545. Such a large value of  $\alpha$  may be in conflict with the principle of energy conservation.

The velocity dispersion adopted for the magnitude of the kick velocity imparted to the neutron star at birth determines the spread of the orbital periods after the supernova explosion of the primary. Small velocity dispersions lead to a narrow distribution of orbital periods close to the upper limit beyond which the binary is disrupted by the supernova explosion, while larger velocity dispersions produce a larger spread with more systems at shorter orbital periods [see Fig. 7 in Kalogera (1996)]. This tendency becomes particularly clear if one compares the orbital period distribution in the absence of kicks (model K0) with the orbital period distribution in the case of large velocity dispersions

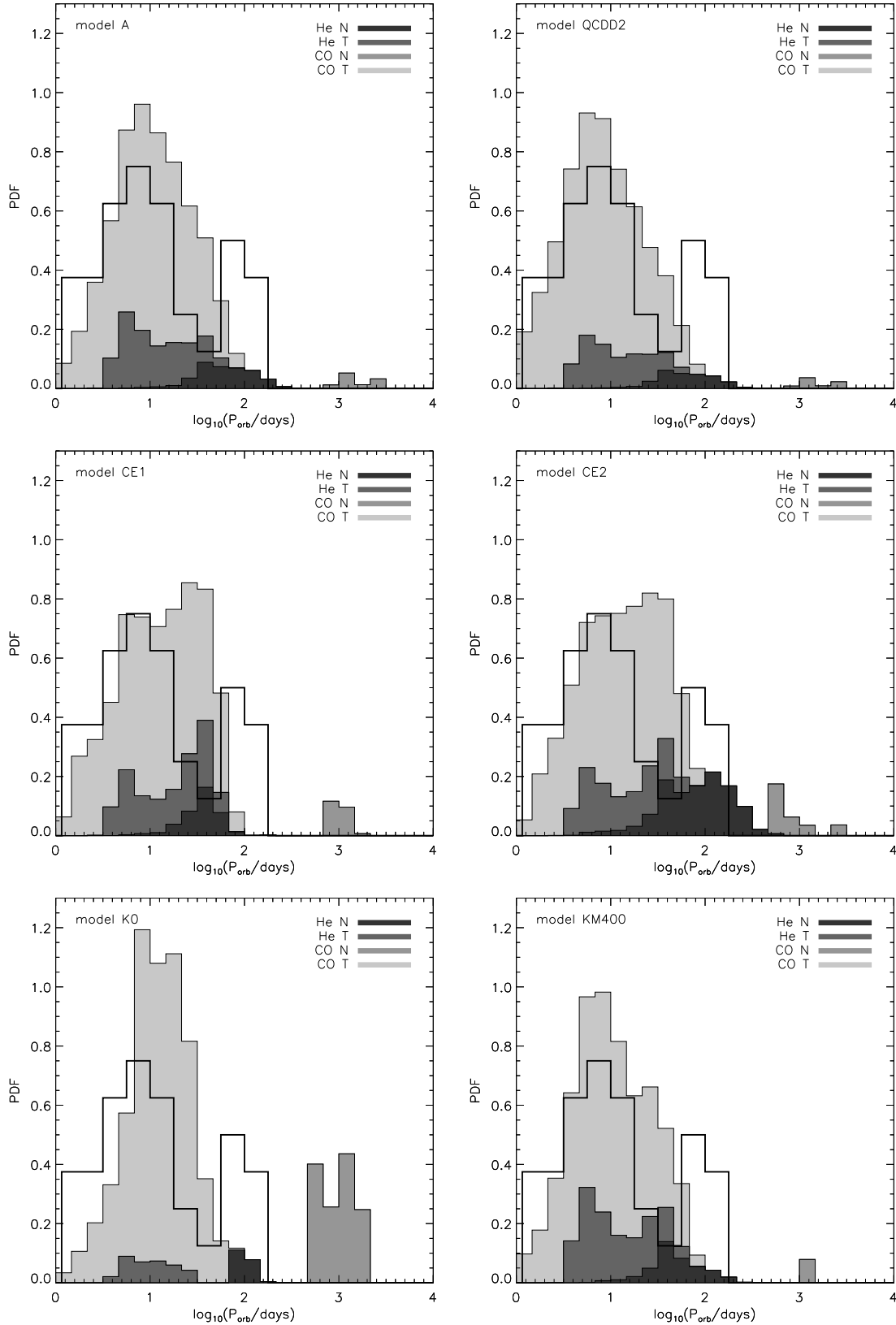


**Figure 8.** The orbital period distribution of the simulated samples of wide BMSPs for the four formation channels considered. The distribution functions of the BMSPs forming through the He N channel are multiplied by a factor of 5, and those of the BMSPs forming through the CO N channel by a factor of 100. The black solid line represents the orbital period distribution of the observed BMSPs listed in Table 1.

(model KM400). The comparison with the observed long orbital period peak is most satisfactory in the absence of kicks or when the kick velocity dispersion is not excessively high ( $\sigma \lesssim 100$  km/s).

Increasing the amount of mass that can be accreted by the neutron star from  $0.2 M_{\odot}$  to  $0.6 M_{\odot}$  does not significantly change the orbital period distribution of the BMSPs. In the limiting case of conservative mass transfer (not shown), the peak in the distribution is located around the orbital period of 15 days, which is far too short in comparison to the position of the long-period peak in the observed distribution. Systems with longer orbital periods do not appear in the conservative case because their progenitors have donor stars with masses below  $0.9 M_{\odot}$ , which evolve too slowly to fill their Roche lobe within the imposed age limit of 15 Gyr. Changes in the critical mass ratio for the delayed dynamical instability, finally, do not influence the orbital period distribution for systems evolving through this formation channel because the mass ratio of the progenitor systems at the onset of Roche-lobe overflow is always well below the critical mass ratio (see Fig. 6).

In all models considered, few systems are found with orbital periods longer than  $\sim 200$  days. The decrease of the simulated distribution functions at longer orbital periods is, however, a lot less sharp than the decrease in the observed orbital period distribution, except for model K0. The paucity of systems beyond  $\sim 200$  days also occurred in a test simulation where we allowed the neutron star to accrete at the Eddington rate without imposing an upper limit on the amount of mass that can be accreted. The lack of long period systems in the simulated orbital period distributions is therefore not due to the inefficiency of the accretion process resulting from, e.g., disc instabilities as proposed by Ritter & King (2002), but due to the upper limit on the post-supernova orbital periods which in turn is caused by the upper limit on the initial orbital periods (see Figs. 5 and 6 and the associated discussion in Sect. 4). The upper limit is preserved by the mass-transfer process after the supernova explosion due to the limited range of donor star masses ( $0.9 M_{\odot} \lesssim M_2 \lesssim 1.3 M_{\odot}$ ) available for stable nuclear timescale mass transfer. This is consistent with the results presented by Podsiadlowski, Rappaport & Pfahl (2001).

The orbital period distribution of the BMSPs descending from the evolutionary channel He T (dark grey) typically has a peak at orbital periods smaller than 10 days, followed by a long-period tail which can extend up to  $\sim 60$  days. The position of the peak is very robust with regard to changes in the common-envelope efficiency and the kick velocity dispersion, except in the case of the low envelope ejection efficiency  $\alpha = 0.2$  when the simulated distribution has a significant secondary peak located in the period gap of the observed orbital period distribution.

Variations in the assumptions regarding the mass-accretion rate onto the neutron star again do not significantly influence the distribution, except in the limiting case of conservative mass transfer (not shown). In the latter case, mass accretion from donor stars more massive than  $\sim 1.8 M_{\odot}$  pushes the mass of the neutron star over the imposed upper limit of  $3.0 M_{\odot}$ , causing the neutron star to collapse into a black hole. Since mass transfer for systems evolving through this formation channel initially takes place on a thermal timescale, the orbital period of the system at the end of the

Roche-lobe overflow phase increases with decreasing mass of the donor star at the onset of Roche-lobe overflow (e.g. King & Ritter 1999). Hence, the lack of systems with initial donor star masses above  $\sim 1.8 M_{\odot}$  in model C shifts the peak in the orbital period distribution towards orbital periods that are too long in comparison to the position of the short orbital period peak in the observed distribution. A similar shift takes place when the critical mass ratio for the delayed dynamical instability is decreased from the values tabulated by Hjellming (1989) to  $q_{c,ddi} = 2.5$  (model QCDD, not shown).

The BMSPs forming through the evolutionary channel CO T (light grey) generally dominate the simulated orbital period distribution at short orbital periods. The distribution function shows a peak around  $\sim 10$  days, and a cut-off at  $\sim 100$  days. In the conservative mass-transfer model (not shown), neutron stars with Roche-lobe filling companions more massive than  $\sim 1.8 M_{\odot}$  again collapse into a black hole, so that no BMSPs are formed through this channel (see also Fig. 6). A decrease of the critical mass ratio for the delayed dynamical instability to  $q_{c,ddi} = 2.5$  shifts the peak of the distribution function towards the period gap of the observed orbital period distribution. All other model parameters do not significantly affect the orbital period distribution of the BMSPs forming through this channel.

Comparison of the simulated orbital period distributions resulting from the formation channels He N and CO T shows that for comparable post-supernova orbital periods, case B Roche-lobe overflow from a low-mass donor star can lead to very different final orbital periods than case B Roche-lobe overflow from an intermediate-mass donor star. This behaviour was put forward by Taam et al. (2000) as a possible explanation for the period gap in the orbital period distribution of the observed Galactic BMSPs. We note that we here also find a contribution to the distribution function below the period gap from systems with intermediate-mass donors evolving through an initial thermal-timescale case A mass-transfer phase followed by a stable case A/case B Roche-lobe overflow phase.

Systems evolving into BMSPs through the formation channel CO N (medium grey) typically have orbital periods around  $\sim 1000$  days and provide the smallest contribution to the total number of BMSPs in our simulated samples. The contribution of these systems to the total population of wide BMSPs is largest for kick velocities with a dispersion of  $\sigma \sim 50$  km/s. It is however clear that the orbital periods of these BMSPs are too long to contribute to the orbital period distribution of the observed Galactic BMSPs listed in Table 1. We therefore did not consider these systems in more detail for the present investigation.

### 5.3 Relative contributions

The relative contributions of the four formation channels to the total population of wide BMSPs are given in Table 3 for each of the models considered in our investigation. For comparison, the relative contributions to the observed orbital period distribution of systems below and above the period gap are about 75% and 25%, respectively.

The simulated populations of wide BMSPs are dominated by the systems forming through the evolutionary channel CO T, except when mass transfer is treated conser-

**Table 3.** Relative contributions of the four formation channels considered to the total population of wide BMSPs in the case of the initial mass ratio distribution given by Eq. (4).

model	He N	He T	CO T	CO N
A	1.29%	17.90%	80.79%	0.02%
CE1	1.33%	19.42%	79.21%	0.04%
CE2	3.87%	17.63%	78.46%	0.05%
K0	0.65%	5.93%	93.20%	0.22%
KM50	0.23%	3.10%	96.28%	0.39%
KM100	0.53%	6.55%	92.86%	0.05%
KM400	1.43%	21.78%	76.78%	0.01%
NS2	0.79%	15.80%	83.40%	0.01%
QCDD	6.24%	23.10%	70.56%	0.10%
QCDD2	0.90%	13.21%	85.88%	0.01%
C	32.02%	67.37%	0.00%	0.61%

**Table 4.** As Table 3, but with a lower limit  $\Delta M_{\text{NS}} = 0.05 M_{\odot}$  imposed on the mass that needs to be accreted by the neutron star in order to be spun up to a millisecond pulsar.

model	He N	He T	CO T	CO N
A	5.64%	78.08%	16.28%	0.01%
CE1	4.52%	65.77%	29.70%	0.02%
CE2	14.50%	66.05%	19.31%	0.14%
K0	9.59%	87.87%	1.54%	0.99%
KM50	6.48%	87.72%	2.39%	3.40%
KM100	6.24%	76.82%	16.70%	0.24%
KM400	5.22%	79.31%	15.47%	0.00%
NS2	3.81%	76.12%	20.05%	0.01%
QCDD	13.25%	49.05%	37.68%	0.02%
QCDD2	5.37%	79.11%	15.51%	0.01%
C	32.03%	67.40%	0.00%	0.57%

vatively. However, due to the high mass-transfer rates inherent to donor stars located in the Hertzsprung gap, the question may be raised whether neutron stars in binaries evolving through this evolutionary channel can accrete enough matter to be spun up to a millisecond pulsar or not. If we impose a lower limit of  $0.05 M_{\odot}$  on the mass that needs to be accreted by the neutron star (see, e.g., Burderi et al. 1999), only binaries with donor stars initially less massive than  $\sim 2.8 M_{\odot}$  end up as BMSPs. The contributions of the four formation channels to the population of wide BMSPs then change as indicated in Table 4, so that the dominant contribution now stems from the systems evolving through the evolutionary channel He T. The contribution of the systems forming through the evolutionary channel CO T decreases even further if a lower limit of  $0.1 M_{\odot}$  is imposed on the mass that needs to be accreted by the neutron star. In this case, the mass of the donor star at the onset of Roche-lobe overflow must be smaller than about  $2.4 M_{\odot}$  for the binary to end up as a BMSP.

The relative contributions of the four formation channels also depend on the distribution adopted for the mass ratio of the binaries at the start of their evolution. Increasing the weight of binaries with smaller initial mass ratios results in a larger fraction of systems evolving through the evolutionary channel He N, so that more BMSPs are formed with longer orbital periods. Increasing the weight of binaries with larger initial mass ratios has the opposite effect. For illustra-

**Table 5.** As Table 3, but with an initial mass ratio distribution  $n(q) = 1/q$ , for  $0 < q \leq 1$ .

model	He N	He T	CO T	CO N
A	4.41%	18.72%	76.84%	0.04%
CE1	3.77%	21.46%	74.71%	0.07%
CE2	9.65%	18.99%	71.24%	0.12%
K0	2.16%	6.29%	91.02%	0.53%
KM50	0.80%	3.55%	94.65%	1.01%
KM100	2.11%	7.05%	90.71%	0.13%
KM400	4.95%	24.34%	70.69%	0.03%
NS2	2.74%	15.82%	81.41%	0.03%
QCDD	14.37%	22.57%	62.92%	0.14%
QCDD2	3.26%	14.63%	82.08%	0.03%
C	37.39%	62.06%	0.00%	0.55%

**Table 6.** As Table 3, but with the initial mass of both the primary and the secondary weighted independently according to the initial mass function given by Eq. (3).

model	He N	He T	CO T	CO N
A	21.73%	18.25%	59.85%	0.18%
CE1	15.39%	24.15%	60.19%	0.26%
CE2	37.29%	16.56%	45.72%	0.43%
K0	12.60%	5.53%	78.12%	3.75%
KM50	5.19%	3.48%	85.54%	5.80%
KM100	13.10%	6.88%	79.32%	0.70%
KM400	22.36%	24.24%	53.24%	0.16%
NS2	15.24%	15.07%	69.54%	0.15%
QCDD	41.38%	18.62%	39.61%	0.39%
QCDD2	18.12%	15.87%	65.86%	0.15%
C	47.73%	51.45%	0.00%	0.81%

tion, the relative contributions in the case of the mass ratio distribution  $n(q) = 1/q$ , for  $0 < q \leq 1$ , are given in Table 5. In this case, the relative contributions of the systems evolving through the evolutionary channel He N approximately increase by a factor of 3. The overall behaviour of the orbital period distributions associated with the four formation channels is similar to that described in Sect. 5.2.

As a test, we also considered the case where the mass of the secondary is weighted independently from the mass of the primary according to the initial mass function given by Eq. (3). For the models considered, the corresponding orbital period distributions only show a peak at short orbital periods if no kicks are imparted to the neutron star at birth or if the velocity dispersion of the Maxwellian kicks is small ( $\sigma \lesssim 50$  km/s). However, as can be seen from Table 6, the contribution of the systems forming through the evolutionary channel CO N is then significantly too large in comparison to the observed orbital period distribution, so that an independent choice of the mass of both the primary and the secondary from the adopted initial mass function seems unlikely in this context.

#### 5.4 A 'best-fit' solution?

From the results presented in the previous subsections, it is clear that there are still too many uncertainties in some phases of stellar and binary evolution to come up with a unique set of input parameters giving the best possible rep-

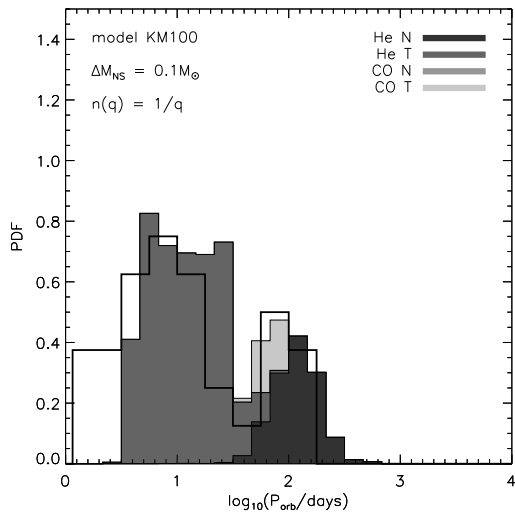


**Figure 9.** The simulated orbital period distribution for model KM100 combined with a lower limit  $\Delta M_{\text{NS}} = 0.1 M_{\odot}$  for the mass that needs to be accreted to spin the neutron star up to millisecond periods and a mass ratio distribution  $n(q) = 1/q$ , for  $0 < q \leq 1$ . The black solid line has the same meaning as in Fig. 8.

resentation of the observed orbital period distribution. An example of a possible combination of input parameters reproducing the main features of the observed distribution is shown in Fig. 9. The simulated distribution is obtained from combining model KM100 with a lower limit  $\Delta M_{\text{NS}} = 0.1 M_{\odot}$  for the mass that needs to be accreted to spin the neutron star up to millisecond periods and a mass ratio distribution  $n(q) = 1/q$ , for  $0 < q \leq 1$ . Since systems forming through the CO N channel only accrete about  $0.05 M_{\odot}$ , they here do not meet the criteria to be classified as BMSPs.

The combination of parameters reproduces the observed short- and long-period peaks as well as the observed period gap, but it fails to reproduce the BMSPs with orbital periods between 1 and 3 days. A possible reason is that the progenitors of these systems are likely to converge during the post-supernova mass-transfer phase, so that they evolve through a different evolutionary channel than those discussed here. The model furthermore only predicts BMSPs containing carbon/oxygen white dwarfs at orbital periods above the period gap, which may pose a problem to explain some of the observed systems with more massive white dwarfs and orbital periods shorter than 20 days (see Fig. 7). This potential inconsistency could be resolved if the uncertainties in the accretion process onto neutron stars during the rapid thermal-timescale mass-transfer phase of the systems evolving through the CO T channel is better understood.

The relative contributions of the systems forming through the He T, He N, and CO T channels are 72.51%, 21.65%, and 5.84%, respectively, which agrees fairly well with the relative number of systems below and above the period gap in the observed orbital period distribution. The agreement is even better if the observed distribution is restricted to orbital periods longer than 3 days, in which case 70% of the observed systems have orbital periods below the gap and 30% have orbital periods above the gap.

## 6 CONCLUDING REMARKS

We have investigated the formation of wide BMSPs through four evolutionary channels using a rapid binary evolution code based on the analytical approximation formulae for the evolution of single stars derived by Hurley et al. (2000).

In three of the channels, dynamically unstable mass transfer from the primary prior to the supernova explosion results in a common-envelope phase during which the orbital separation is reduced and the helium core of the primary is exposed as a naked helium star. The primary continues its evolution until it becomes a neutron star in a type Ib/c supernova explosion. The further evolution depends on the mass of the secondary and on the post-supernova orbital period after circularisation:

- If the mass of the secondary is smaller than  $\sim 1.6 M_{\odot}$ , the binary undergoes a stable case B mass-transfer phase when the secondary reaches the giant branch. The binary becomes a BMSP consisting of a rapidly rotating neutron star orbiting a helium white dwarf with an orbital period determined by the mass of the white dwarf.
- If the mass of the secondary is larger than  $\sim 1.6 M_{\odot}$  and the orbital period shorter than  $\sim 2.5$  days, the binary undergoes a thermal-timescale case A mass-transfer phase, followed by a stable phase of case A and/or case B Roche-lobe overflow. The system again evolves into a BMSP containing a helium white dwarf whose mass determines the orbital period.
- If the mass of the secondary is larger than  $\sim 1.6 M_{\odot}$  and the orbital period longer than  $\sim 2.5$  days, the binary undergoes a thermal-timescale case B mass-transfer phase when the secondary crosses the Hertzsprung gap. The system evolves into a binary containing a neutron star and a carbon/oxygen white dwarf without developing a tight correlation between the orbital period and the mass of the white dwarf. The accretion onto the neutron star in these binaries may not be efficient enough to spin them up to millisecond pulsars.

The fourth evolutionary channel corresponds to the direct supernova mechanism where no interaction between the binary components takes place until the primary gives birth to a neutron star in a type II supernova explosion on the AGB. If the resulting post-supernova orbit is wide enough to avoid any interaction until the secondary becomes an AGB star, stable case C mass transfer leads to the formation of a BMSP containing a carbon/oxygen white dwarf whose mass is correlated with the orbital period.

Our main goal in this investigation was to compare the orbital period distribution of simulated samples of BMSPs resulting from different sets of input parameters for the binary evolution calculations with the orbital period distribution of wide BMSPs observed in the Galactic disc. The observed long orbital period peak is identified with the BMSPs containing a helium white dwarf whose progenitor underwent a mass-transfer phase that was stable at all times. The observed short orbital period peak on the other hand is identified with the BMSPs containing a helium white dwarf whose progenitor evolved through a thermal-timescale mass-transfer phase on the main sequence or in the Hertzsprung gap.

The simulated distribution functions all show a rapid

decrease for orbital periods longer than 200 days, irrespective of the accretion efficiency of neutron stars. The lack of longer period systems is a consequence of the upper limit on the initial orbital periods beyond which the binary remains detached instead of going through a common-envelope phase prior to the supernova explosion of the primary. The agreement between the simulated and the observed orbital period distributions is best for models with highly non-conservative mass transfer, common-envelope efficiencies equal to or larger than unity, a critical mass ratio for the delayed dynamical instability larger than 3, and no or moderate supernova kicks at the birth of the neutron star.

The first results of the population synthesis study presented here are encouraging, but many uncertainties remain to be solved. The lack of BMSPs containing carbon/oxygen white dwarfs at orbital periods shorter than 20 days in our 'best-fit' solution, for instance, surely poses a problem that needs to be resolved. A more detailed treatment of the accretion process onto neutron stars and the potential effects of pulsar turn-on, evaporation, and spin-down are of particular importance to improve the population synthesis study of wide BMSPs. Preliminary calculations also reveal a dependency of the orbital period distribution on the mass-loss rates from stellar winds, but the results are still inconclusive.

Furthermore, our population synthesis study implicitly incorporates a model for the Galactic population of neutron star X-ray binaries. The long-standing apparent conflict between the observationally implied birth rate of BMSPs and their LMXB progenitors (e.g. Ruderman, Shaham & Tavani 1989; Podsiadlowski et al. 2002 and references therein) may point towards non-standard evolutionary effects in the X-ray binary phase which are not considered in our study. It is therefore desirable to consider the populations of LMXBs and BMSPs simultaneously.

We will address these matters in more detail in future investigations.

## ACKNOWLEDGEMENTS

We are grateful to Hans Ritter for providing the data of the observed BMSPs and to Jarrod Hurley, Onno Pols, and Chris Tout for sharing their SSE software package and a copy of the paper describing their binary evolution algorithm prior to publication. We also thank Jarrod Hurley, Chris Tout, Simon Portegies-Zwart, and Firoza Sutaria for useful discussions. We thank the referee, Philipp Podsiadlowski, for useful comments. This research was supported by the British Particle Physics and Astronomy Research Council (PPARC).

## APPENDIX A: ACCRETION ONTO NEUTRON STARS

In this appendix, we briefly outline the treatment of mass accretion by neutron stars in semi-detached binaries adopted in our binary evolution code. We assume mass transfer to be non-conservative and denote by  $\gamma$  the fraction of the transferred mass that is lost from the system. The mass-accretion rate onto the neutron star is then related to the mass-transfer rate from the donor star by

$$\dot{M}_{\text{NS}} = (1 - \gamma)|\dot{M}_2|, \quad (\text{A1})$$

where  $M_{\text{NS}}$  is the mass of the neutron star, and  $M_2$  the mass of the Roche-lobe overflowing companion.

If we furthermore assume that the neutron star accretes a maximum mass  $(\Delta M_{\text{NS}})_{\text{max}}$  during the mass transfer process, the average mass-accretion rate onto the neutron star is given by

$$\dot{M}_{\text{NS}} = (\Delta M_{\text{NS}})_{\text{max}} \frac{|\dot{M}_2|}{M_2}, \quad (\text{A2})$$

so that

$$\gamma = 1 - \frac{(\Delta M_{\text{NS}})_{\text{max}}}{M_2}. \quad (\text{A3})$$

In order to ensure that the neutron star accretes not more than  $(\Delta M_{\text{NS}})_{\text{max}}$ , we then adopt the artificial rate given by (A2) as the mass-accretion rate onto the neutron star.

## REFERENCES

- Bhattacharya, D., van den Heuvel, E.P.J. 1991, Phys. Rep. 203, 1
- Burderi, L., Possenti, A., Colpi, M., di Salvo, T., D'Amico, N. 1999, ApJ 519, 285
- Dewi, J.D.M., Pols, O.R., Savonije, G.J., van den Heuvel, E.P.J. 2002, MNRAS 331, 1027
- Dewi, J.D.M., Tauris, T.M. 2000, A&A 360, 1043
- Dewi, J.D.M., Tauris, T.M. 2001, in Evolution of Binary and Multiple Star Systems; A Meeting in Celebration of Peter Eggleton's 60th Birthday, Eds. Podsiadlowski, Ph., Rappaport, S., King, A.R., D'Antona, F., Burderi, L., ASP Conf. Ser. 229, 255
- Eggleton, P.P., Fitchett, M.J., Tout, C.A. 1989, ApJ 347, 998
- Ergma, E., Sarna, M.J. 1996, MNRAS 280, 1000
- Ergma, E., Sarna, M.J., Antipova, J. 1998, MNRAS 300, 352
- Hjellming, M.S. 1989, Rapid mass transfer in binary systems, Ph.D. Thesis Illinois University at Urbana-Champaign, Savoy
- Hurley, J.R., Pols, O.R., Tout, C.A. 2000, MNRAS 315, 543
- Hurley, J.R., O.R., Tout, C.A., Pols, O.R. 2002, MNRAS 329, 897
- Joss, P.C., Rappaport, S., Lewis, W. 1987, ApJ 319, 180
- Kalogera, V., 1996, ApJ 471, 352
- Kalogera, V., 1998, ApJ 493, 368
- Kalogera, V., Kolb, U., King, A.R. 1998, ApJ 504, 967
- Kalogera, V., Webbink, R.F. 1998, ApJ 493, 351
- King, A.R., Ritter, H. 1999, MNRAS 309, 253
- Kolb, U., Davies, M.B., King, A., Ritter, H. 2000, MNRAS 317, 438
- Kolb, U., Rappaport, S., Schenker, K., Howell, S. 2001, ApJ 563, 958
- de Kool, M. 1992, A&A 261, 188
- Kroupa, P., Tout, C.A., Gilmore G. 1993, MNRAS 262, 545
- Kudritzki, R.P., Reimers, D. 1978, A&A 70, 227
- Kudritzki, R.P., Pauldrach, A., Puls, J., Abbott, D.C. 1989, A&A 219, 205
- Li, X.-D. 2002, ApJ 564, 930
- Nieuwenhuizen, H., de Jager, C. 1990, A&A 231, 134
- Phinney, E.S., Kulkarni, S.R. 1994, ARA&A 32, 591
- Podsiadlowski, Ph., Rappaport, S. 2000, ApJ 529, 946
- Podsiadlowski, P., Rappaport, S., Pfahl, E.D. 2001, in The Influence of Binaries on Stellar Population Studies, Ed. D. Vanbeveren, ASSL 264, 355
- Podsiadlowski, P., Rappaport, S., Pfahl, E.D. 2002, ApJ 565, 1107
- Politano, M.J. 1996, ApJ 465, 338
- Pylyser, E., Savonije, G.J. 1988, A&A 191, 57
- Pylyser, E., Savonije, G.J. 1989, A&A 208, 52

- Rappaport, S., Podsiadlowski, Ph., Joss, P.C., di Stefano, R., Han, Z. 1995, MNRAS 273, 731
- Rappaport, S., Putney, A., Verbunt, F. 1989, ApJ 345, 210
- Rasio, F.A., Pfahl, E.D., Rappaport, S. 2000, ApJ 532, L47
- Ritter, H. 1999, MNRAS 309, 360
- Ritter, H., King, A., 2002, in *The Physics of Cataclysmic Variables and Related Objects*, Eds. Gänsicke B.T., Beuermann K., Reinsch K., ASP Conf. Ser. 261, 531
- Ruderman, M., Shaham, J., Tavani, M. 1989, ApJ 336, 507
- Savonije, G. J. 1987, Nature 325, 416
- Taam, R.E., King, A.R., Ritter, H. 2000, ApJ 541, 329
- Tauris, T.M. 1996, A&A 315, 453
- Tauris, T.M., Bailes, M. 1996, A&A 315, 432
- Tauris, T.M., Savonije, G.J. 1999, A&A 350, 928
- Tauris, T.M., Sennels, T. 2000, A&A 355, 236
- Tauris, T.M., van den Heuvel, E.P.J., Savonije, G.J. 2000, ApJ 530, L93
- Thorsett, S.E., Chakrabarty, D. 1999, ApJ 512, 288
- Vassiliadis, E., Wood, P.R. 1993, ApJ 413, 641
- Webbink, R.F. 1985, in Pringle J.E., Wade R.A., Eds. *Interacting Binary Stars*, Cambridge University Press, Cambridge

This paper has been typeset from a  $\text{\TeX}/\text{\LaTeX}$  file prepared by the author.